

Structure and Luminescence Properties of [Re(4,7-dimethyl-1,10-phenanthroline)(CO)₃py]⁺ in a Solid Matrix

Lynne Wallace,[†] Clifton Woods,[‡] and D. Paul Rillema^{*,§}

The Research School of Chemistry, The Australian National University, Canberra, ACT 0200, Australia, Department of Chemistry, The University of Tennessee, Knoxville, Tennessee 37996, and Department of Chemistry, The University of North Carolina at Charlotte, Charlotte, North Carolina 28223

Received March 6, 1995[⊗]

The low-temperature luminescence properties of [Re(4,7-Me₂phen)(CO)₃py]⁺ (4,7-Me₂phen = 4,7-dimethyl-1,10-phenanthroline, py = pyridine) as a crystal or in ethanol–methanol glass are reported, together with a crystal structure of the complex as its perchlorate salt. The complex [Re(4,7-Me₂phen)(CO)₃py](ClO₄) crystallizes in the space group *Pna*2₁ with *a* = 16.262(4) Å, *b* = 12.721(3) Å, *c* = 10.814(2) Å, and *Z* = 4. The geometry is facial and the Re–N(4,7-Me₂phen) bond lengths are 2.13(2) and 2.24(2) Å, the Re–N(py) bond distance is 2.15(2) Å, and the Re–C(CO) bond distances are 1.93(3), 1.87(3), and 1.90(2) Å. Single-crystal absorption and luminescence spectra at temperatures below 6 K show that the emitting state in this environment is triplet ligand-centered (³LC). In an ethanol–methanol glass, the luminescence spectra indicate that a largely ³LC assignment is also appropriate in this matrix; however lifetime measurements provide some evidence for a contribution from the nearby triplet metal-to-ligand charge-transfer (³MLCT) state. Measurements of the Zeeman effect in both environments confirm these conclusions.

Introduction

There are by now many examples of Re(I) tricarbonyl complexes which display anomalous luminescence properties such as multiexponential decay profiles and time-dependent emission spectra.^{1–9} Usually the properties of the complexes have been studied by conventional spectroscopic methods (such as broad-band emission and absorption spectra and lifetime measurements) but have seldom been examined at very low temperatures (4.2 K) or subjected to selective spectroscopies.

In most cases, the behavior outlined above has been attributed to the occurrence of simultaneous emission from spin-forbidden metal-to-ligand charge transfer (³MLCT) and spin-forbidden ligand-centered (³LC) states which are very close in energy. Usually, ³LC excited states are longer-lived (50 μs–1 ms at 77 K) and the luminescence spectra are structured. Luminescences from ³MLCT states typically have shorter lifetimes (several microseconds at 77 K) and inhomogeneous line widths are somewhat broader. However in some cases these guidelines can be insufficient, and more definitive methods of determining the orbital and spin character of the luminescence are required.

Luminescence line narrowing spectroscopy (LLN) is one method which can aid in the classification of excited states.¹⁰ This technique employs narrow-band laser excitation into a low-energy absorption feature, so that emission occurs *only* from those species within the inhomogeneous line width which absorb exactly at that wavelength. One can observe the resulting luminescence either resonantly (at the laser wavelength) or nonresonantly (at wavelengths shifted from the laser). The line widths of luminescence spectra observed in this way are usually much sharper, due to the reduction in the spread of emission energies. ³LC luminescence is usually readily narrowed, since the features are normally well resolved to begin with. This is because the inhomogeneous broadening tends to be less, in comparison with ³MLCT emission. Also, the electronic origin ordinarily carries most of the intensity for excitations involving ³LC states, and in contrast the vibrational sideband is relatively weak. ³MLCT excitations, on the other hand, seem to carry very little intensity in the electronic origin,¹¹ and this combined with the broader line widths means that MLCT excitations cannot normally be narrowed in amorphous hosts, although this has been achieved in crystal samples.^{12,13} In the case of an iridium(III) complex, Ir(5,6-Me₂phen)₂Cl₂⁺ (5,6-Me₂phen = 5,6-dimethyl-1,10-phenanthroline), which showed behavior associated with simultaneous emission from ³MLCT and ³LC states, resonant line-narrowing experiments at 4.2 K were able to demonstrate conclusively the ³LC assignment of the emission.¹⁴ More detailed information regarding the character of the emitting state was provided by examining the effect of an applied magnetic field on the appearance of the luminescence spectra. From the observed pattern of the Zeeman levels of the origin, it was found that the zero-field splittings of the ³LC state were rather large for a pure spin triplet, and it was concluded that the ³LC state was perturbed by the nearby ³MLCT state. In another example, complexes which showed apparently ³LC

[†] The Australian National University.

[‡] The University of Tennessee.

[§] The University of North Carolina at Charlotte. Present address: Department of Chemistry, Wichita State University, Wichita, KS 67260-0051.

[⊗] Abstract published in *Advance ACS Abstracts*, May 1, 1995.

- (1) Wallace, L.; Rillema, D. P. *Inorg. Chem.* **1993**, *32*, 3836.
- (2) Sacksteder, L.; Lee, M.; Demas, J. N.; DeGraff, B. A. *J. Am. Chem. Soc.* **1993**, *115*, 8230.
- (3) Leasure, R. M.; Sacksteder, L.; Nesselrodt, D.; Reitz, G. A.; Demas, J. N.; DeGraff, B. A. *Inorg. Chem.* **1991**, *30*, 3722.
- (4) Sacksteder, L.; Zipp, A. P.; Brown, E. A.; Streich, J.; Demas, J. N.; DeGraff, B. A. *Inorg. Chem.* **1990**, *29*, 4335.
- (5) Shaw, J. R.; Schmehl, R. H. *J. Am. Chem. Soc.* **1991**, *113*, 389.
- (6) Juris, A.; Campagna, S.; Bidd, I.; Lehn, J.-M.; Zeissel, R. *Inorg. Chem.* **1988**, *27*, 4007.
- (7) Fredericks, S. M.; Luong, J. C.; Wrighton, M. S. *J. Am. Chem. Soc.* **1979**, *101*, 7415.
- (8) Giordano, P. J.; Fredericks, S. M.; Wrighton, M. S.; Morse, D. L. *J. Am. Chem. Soc.* **1978**, *100*, 2257.
- (9) Wrighton, M. S.; Morse, D. L. *J. Am. Chem. Soc.* **1974**, *96*, 998.

(10) Riesen, H.; Krausz, E. *Comments Inorg. Chem.* **1993**, *14*, 323.

(11) Krausz, E.; Ferguson, J. *Prog. Inorg. Chem.* **1989**, *37*, 293.

(12) Riesen, H.; Krausz, E. *Chem. Phys. Lett.* **1993**, *212*, 347.

(13) Riesen, H.; Krausz, E. *J. Chem. Phys.* **1993**, *99*, 7614.

(14) Riesen, H.; Wallace, L.; Krausz, E. *J. Phys. Chem.* **1992**, *96*, 3621.

emission, $[\text{Ir}(\text{bpy})_2(\text{acac})]^{2+}$ and $[\text{Ir}(\text{bpy})_2(\text{MeOH})_2]^{3+}$, were established as $^3\text{MLCT}$ emitters using narrowing techniques.¹⁵

For rhenium(I) polypyridyl complexes, the differences in behavior between $^3\text{MLCT}$ and ^3LC emitters are usually so obvious as to put the assignment of the emitting state beyond question. However, there are now many examples of the kind of behavior outlined above, where one can observe both types of emission occurring simultaneously, and considering the possibility of perturbed $^3\text{MLCT}$ or ^3LC states, the differences may not always be evident.

Recently we reported the complex luminescence properties of a series of rhenium(I) polypyridyl complexes.¹ In solution, the complexes $[\text{Re}(\text{L-L})(\text{CO})_3\text{py}]^+$ (L-L = 3,4,7,8-Me₄phen, 4,7-Me₂phen, 5,6-Me₂phen, 2,9-Me₂phen, phen, 5-Phphen, 4,7-Ph₂phen, 2,9-Me₂-4,7-Ph₂phen) exhibited luminescence that was typical of charge-transfer excited states, but at 77 K in an ethanol-methanol glass there was clearly some ^3LC character in the emission.

We have now studied one of the complexes included in ref 1, $[\text{Re}(4,7\text{-Me}_2\text{phen})(\text{CO})_3\text{py}]^+$, in more detail. First, in order to reduce complications caused by sample inhomogeneity, we have examined the photophysics of a single crystal of the complex. A crystal structure has also been obtained. Second, we have employed luminescence line-narrowing techniques, in addition to conventional spectroscopic methods, to probe the excited-state characteristics of the complex in a low-temperature ethanol-methanol glass (EM). Finally, both the crystal and glassy samples were subjected to a magnetic field at 4.2 K in order to observe the Zeeman effect on the emitting state in either matrix.

Experimental Section

General Procedures. The preparation of $[\text{Re}(4,7\text{-Me}_2\text{phen})(\text{CO})_3\text{py}]^+$ has been described previously.¹ Crystals were grown from saturated solutions of the perchlorate salt in ethanol-methanol (4:1 v/v).

Absorption spectra of single crystals were recorded using a single-beam apparatus described elsewhere.¹⁶ For emission lifetime measurements, samples were excited using a Photochemical Research Associates (PRA) Model LN 1000 pulsed N₂ laser, fitted with a PRA LN102 dye laser. Samples were cooled by the flow tube method. In the luminescence and Zeeman measurements, samples were cooled in a BOC superconducting cryomagnet, controlled by an Oxford Instruments power supply, and were excited using different lines of a SpectraPhysics 165 Ar⁺ laser. A chopper was employed for the resonant line-narrowing experiments, running at a speed of 1800 Hz, which corresponds to ≈ 30 μs delay between excitation and detection. The luminescence was dispersed by a Spex 1404 double monochromator and detected by a cooled photomultiplier. The signal was processed by a Stanford Research Systems SR530 lock-in amplifier, and data acquisition was controlled by computer.

Crystal Structure Determination of $[\text{Re}(4,7\text{-Me}_2\text{phen})(\text{CO})_3\text{py}](\text{ClO}_4)$. A yellow-green parallelepiped of dimensions $0.30 \times 0.30 \times 0.20$ mm was selected for structure analysis. X-ray data were collected on a Siemens R 3mV diffractometer using the $\theta-2\theta$ method. A total of 1718 reflections were recorded in the 2θ range $3.5-45^\circ$ using MoK α radiation. Of the 1564 independent reflections, 1147 reflections with $F_o > 6.0\sigma(F_o)$ were used in full-matrix least-squares refinement. Final residuals were $R(F) = 0.0480$ and $R_w(F) = 0.0409$. The data were corrected for Lorentz and polarization effects, and an empirical absorption correction based on the ϕ dependence of five reflections with $\chi \approx 90^\circ$ was applied ($T_{\text{max}}:T_{\text{min}} = 0.952:0.802$). The Re atom was located by the heavy atom method using the SHELXTL PLUS software,¹⁷ and the remaining non-hydrogen atoms were refined

Table 1. Crystallographic Data for $[\text{Re}(4,7\text{-Me}_2\text{phen})(\text{py})(\text{CO})_3]\text{ClO}_4$

$\text{C}_{22}\text{H}_{17}\text{ClN}_3\text{O}_7\text{Re}$	$T = -110^\circ\text{C}$
fw = 657.0	$Z = 4$
$a = 16.262(4) \text{ \AA}$	$\lambda = 0.71069 \text{ \AA}$
$b = 12.721(3) \text{ \AA}$	$d_{\text{calc}} = 1.951 \text{ g/cm}^3$
$c = 10.814(2) \text{ \AA}$	$\mu = 56.7 \text{ cm}^{-1}$
$V = 2237.1(9) \text{ \AA}^3$	$R(F_o)^a = 0.0480$
space group $Pna2_1$	$R_w(F_o)^b = 0.0409$

$$^a R = \sum ||F_o| - |F_c|| / \sum |F_o|. \quad ^b R_w = [\sum w(|F_o| - |F_c|)^2 / \sum w F_o^2]^{1/2}.$$

Table 2. Atomic Coordinates ($\times 10^4$) and Equivalent Isotropic Displacement Coefficients ($\text{\AA}^2 \times 10^3$) for $[\text{Re}(4,7\text{-Me}_2\text{phen})(\text{py})(\text{CO})_3]\text{ClO}_4$

	x	y	z	$U(\text{eq})^a$
Re	598(1)	1029(1)	0	20(1)
Cl	2647(4)	-2430(5)	-587(6)	27(2)
N(2)	-162(12)	2111(16)	-980(18)	13(5)
N(3)	128(12)	2168(16)	1416(19)	20(6)
O(4)	2853(10)	-1646(13)	-1475(15)	33(5)
O(5)	1807(12)	-2270(14)	-276(19)	71(7)
C(2)	965(15)	138(20)	-1261(23)	14(6)
C(3)	-251(13)	37(18)	313(25)	33(7)
C(4)	350(12)	2199(17)	2625(20)	14(6)
C(5)	61(16)	2963(20)	3389(25)	36(7)
C(6)	-460(13)	3766(16)	2967(19)	18(6)
C(7)	-1173(16)	4512(22)	1121(24)	34(7)
C(8)	-1340(13)	4493(17)	-52(49)	42(7)
C(9)	-1139(15)	3618(18)	-2195(24)	25(6)
C(10)	-796(13)	2821(18)	-2796(21)	24(6)
C(11)	-333(14)	2090(19)	-2200(23)	27(7)
C(13)	-336(15)	2905(21)	964(24)	23(7)
C(15)	-661(15)	3743(16)	1704(21)	24(6)
C(16)	-1019(15)	3661(19)	-904(23)	20(6)
C(21)	1765(15)	2513(19)	-1444(22)	21(6)
O(3)	-734(11)	-612(14)	423(16)	58(6)
O(2)	1162(11)	-377(14)	-2081(17)	39(5)
C(18)	2605(15)	3420(19)	484(21)	22(7)
O(7)	3179(13)	-2231(16)	452(20)	69(8)
O(1)	1690(14)	-202(17)	1835(21)	60(6)
O(6)	2776(12)	-3445(15)	-1091(18)	55(6)
N(1)	1550(10)	2182(11)	-266(14)	11(5)
C(1)	1289(17)	261(22)	1141(26)	28(8)
C(19)	2722(17)	3776(22)	-677(24)	31(8)
C(23)	-1711(15)	4407(18)	-2807(22)	36(7)
C(17)	1994(19)	2623(19)	681(22)	21(6)
C(20)	2350(15)	3286(19)	-1666(23)	29(7)
C(22)	-771(15)	4607(20)	3851(24)	41(8)
C(14)	-501(14)	2950(17)	-361(16)	9(6)

^a Equivalent isotropic U defined as one-third of the trace of the orthogonalized U_{ij} tensor.

isotropically. The hydrogen atoms were placed at their calculated positions ($d(\text{C-H}) = 0.96 \text{ \AA}$) which were not refined, but instead the hydrogen atoms were allowed to ride along with their bonded atoms during refinement. The crystallographic data are given in Table 1.

Results

Structure of $[\text{Re}(4,7\text{-Me}_2\text{phen})(\text{CO})_3\text{py}](\text{ClO}_4)$. The atomic positional parameters are given in Table 2, and selected bond angles and distances are given in Table 3. Figure 1 shows an ORTEP drawing of the cation. The coordination geometry of the Re atom is that of a distorted octahedron with a ReN_3C_3 core in a facial arrangement. Two nitrogen atoms belong to the 4,7-Me₂phen ligand and the third belongs to the pyridine ligand. The distortion from octahedral geometry is caused by the small bite angle ($74.0(7)^\circ$) of the 4,7-Me₂phen ligand. Although the two Re-N distances between Re and the 4,7-Me₂phen ligand are 2.13(3) and 2.24(2) \AA , there is no obvious electronic cause for this difference. Thus the Re-N distances to the 4,7-Me₂phen ligand are likely the result of crystal packing phenomena. However, the longest Re-N bond is trans to the

(15) Riesen, H.; Krausz, E. *J. Lumin.* **1994**, *62*, 253.

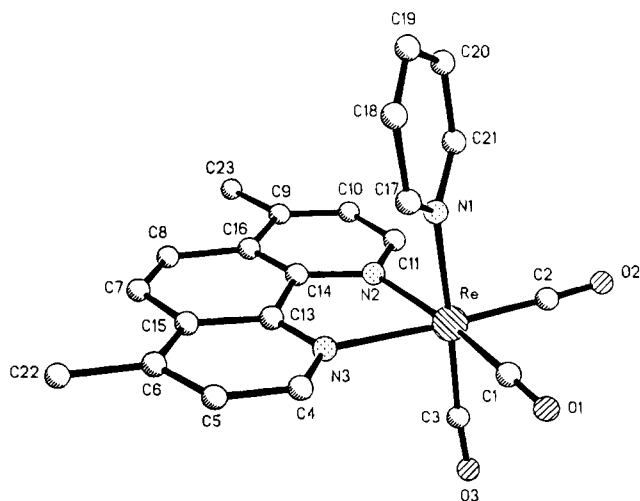
(16) Krausz, E. *Aust. J. Chem.* **1993**, *46*, 1041.

(17) Sheldrick, G. M. *SHELXTL PLUS Structure Solution Package*, Version 4.1; Siemens Analytical Instruments, Inc.: Madison, WI, 1990.

Table 3. Selected Bond Distances and Angles for [Re(4,7-Me₂phen)-(py)(CO)₃ClO₄

Distances (Å)			
Re-N(1)	2.15(2)	Re-C(3)	1.90(2)
Re-N(2)	2.13(2)	C(1)-O(1)	1.16(4)
Re-N(3)	2.24(2)	C(2)-O(2)	1.15(3)
Re-C(1)	1.93(3)	C(3)-O(3)	1.15(3)
Re-C(2)	1.87(3)		

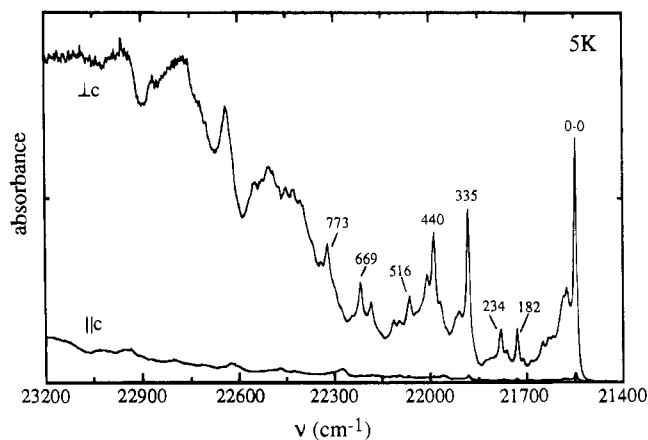
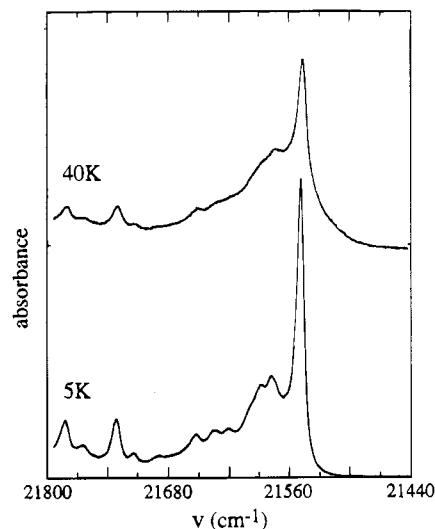
Angles (deg)			
N(2)-Re-N(3)	74.0(7)	N(1)-Re-N(3)	84.0(7)
N(2)-Re-C(2)	102.3(9)	N(1)-Re-C(1)	90.6(9)
N(3)-Re-C(1)	84.0(7)	N(1)-Re-C(2)	94.9(9)
N(1)-Re-N(2)	84.9(7)	N(1)-Re-C(3)	177.2(9)

**Figure 1.** ORTEP drawing of the [Re(4,7-Me₂phen)(CO)₃py]⁺ cation.

shorter Re-C bond, which is consistent with $d\pi-p\pi$ synergism involving the trans N-Re-C linkage. The Re-N(py) bond distance is 2.15 Å. The lack of significant variations in the Re-N bond distance for the 4,7-Me₂phen and py ligands suggests that the donor atoms of the two ligands are similar in electronic nature.

Previously we concluded that Re(I)-N bond distances ranged from 2.13 to 2.21 Å in Re(I) complexes where π bonding between the metal center and nitrogen-donating heterocyclic ligands was important.¹⁸ For [Re(bpm)(CO)₃(MeQ)]²⁺, where bpm is 2,2'-bipyrimidine and MeQ⁺ is the *N*-methyl-4,4'-bipyrimidinium ion, the average Re-N(bpm) distance was 2.17 Å and the Re-N(MeQ⁺) distance was 2.21 Å. Horn and Snow reported average Re-N(bpy) bond distances of 2.14 Å for Re-(bpy)(CO)₃(P₂OF₂),¹⁹ where bpy is 2,2'-bipyridine, and Tikkanen et al. reported Re-N("py") bond lengths of 2.19 Å and a Re-N("naphthyridine") bond length of 2.21 Å for the complex bromotricarbonyl(2,7'-bis(2-pyridyl)-1,8-naphthyridine)rhenium(I).²⁰

Single-Crystal Polarized Absorption Spectra. Figure 2 shows absorption spectra of a single crystal of [Re(4,7-Me₂phen)(CO)₃py]⁺ at 5 K, measured with the light propagating parallel and perpendicular to the crystal *c* axis. There are several narrow absorption lines in the low-energy region which are strongly polarized in the perpendicular (*ab*) plane. The strongest feature is the lowest-energy line at 21548 cm⁻¹; this corresponds to the zero-phonon transition between the ground state and the lowest excited state (ie. the origin). The line width of this transition is 7 cm⁻¹. A high-energy phonon wing occurs at a

**Figure 2.** Absorption spectra of a single crystal of [Re(4,7-Me₂phen)-(CO)₃py](ClO₄), measured parallel and perpendicular to the crystal *c* axis at 5 K. The frequency shifts of major sidelines are indicated.**Figure 3.** Temperature dependence of the origin region of the absorption spectrum of [Re(4,7-Me₂phen)(CO)₃py](ClO₄), in the spectrum measured perpendicular to the crystal *c* axis. Spectra were measured at 5 and 40 K.

shift of 30 cm⁻¹ from the origin, and a similar wing is found for the next strong feature at 21 883 cm⁻¹. Upon warming of the sample to 40 K (Figure 3), the origin loses ca. 50% of its intensity, which has been redistributed into the phonon wing.

The appearance and temperature dependence of the origin region of the spectrum are characteristic of LC transitions. Typically, electronic bands involving ³LC excited states have a substantial fraction of the intensity residing in the electronic origin itself. This is because the ground state and excited state usually differ very little with respect to equilibrium geometry and preferred outer-sphere environment, and the Huang-Rhys parameter (*S*) is therefore very small. The wing at higher energy arises from the coupling of the origin transition to the lattice modes of the host lattice or solvent (phonons). A similar effect operates in luminescence (see below), in this case with the phonon wing occurring at lower energy compared to the zero-phonon line. The distribution of intensity between the origin and phonon wing is given by the Debye-Waller factor, $\alpha = I_{0-0}/(I_{0-0} + I_{pw})$, which can vary between 1 and 0, depending on the chromophore.²¹ The Debye-Waller factor has an inverse dependence on temperature, so that at higher temperatures more

(18) Winslow, L. N.; Rillema, D. P.; Welch, J. H.; Singh, P. *Inorg. Chem.* **1989**, *28*, 1596.

(19) Horn, E.; Snow, M. R. *Aust. J. Chem.* **1980**, *197*, 2369.

(20) Tikkanen, W.; Kaska, W. C.; Moya, S.; Layman, T.; Kane, R. *Inorg. Chim. Acta* **1983**, *76*, L29.

(21) Personov, R. I. In *Spectroscopy and excitation dynamics of condensed molecular systems*; Agranovich, V. M.; Hochstrasser, R. M., Eds.; North-Holland: Amsterdam, 1983.

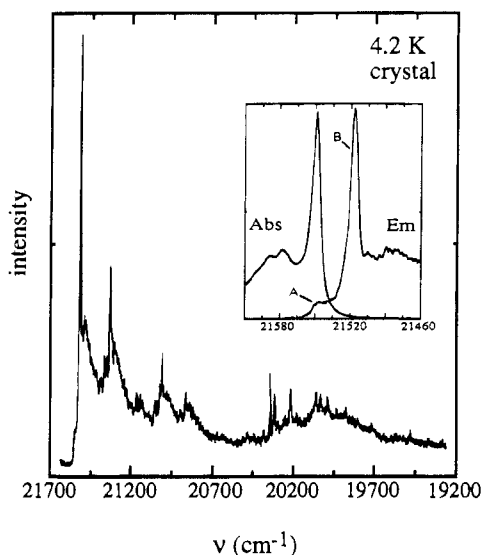


Figure 4. Luminescence spectrum of a single crystal of $[\text{Re}(4,7\text{-Me}_2\text{-phen})(\text{CO})_3\text{py}](\text{ClO}_4)$ at 4.2 K with 454.5 nm excitation. The insert shows the overlap of absorption and emission spectra in the origin region, with A indicating the origin of the bulk material and B indicating the origin of the minority site (see text).

of the intensity is transferred into the phonon wing. This is exemplified by the spectra in Figure 3, for which $\alpha \approx 0.5$ at 5 K and $\alpha \approx 0.3$ at 40 K.

Luminescence of a Single-Crystal. The luminescence spectrum of a single crystal of the title complex at 4.2 K, excited at 454.5 nm, is shown in Figure 4. The 454.5 nm Ar^+ line nearly coincides with the $21\,990\text{ cm}^{-1}$ absorption line of the crystal, and this was the lowest excitation frequency which could still access an absorption feature. Since the sample has not been excited directly into the origin (at 464.1 nm), the observed luminescence spectrum is not narrowed. By far, the most intense feature in the luminescence spectrum is the sharp line at $21\,517\text{ cm}^{-1}$, which has a line width of 7 cm^{-1} . This is followed by a vibrational progression which displays a number of well-resolved sidelines. There is a small narrow feature at $21\,547\text{ cm}^{-1}$, 30 cm^{-1} higher in energy than the strong transition, and this weaker band is resonant with the origin in absorption. Thus the weak feature is the true origin of the bulk material, and most of the observed luminescence therefore occurs from a minority site in the crystal, whose origin corresponds to the intense sharp line and which is trapping the excitation energy by virtue of an energy transfer mechanism within the neat material. The strong origin line has a low-energy phonon wing shifted 30 cm^{-1} , a separation similar to that observed in absorption. Relatively little intensity resides in the vibrational sidelines, and this is what has generally been found at low temperature for other transition-metal complexes displaying ^3LC luminescence, such as $[\text{Ru}(\text{i-biq})_3]^{2+}$ or $[\text{Rh}(\text{phen})_3]^{3+}$.²³

Luminescence in Ethanol–Methanol Glass (EM). The (broad-band) luminescence spectra of the title complex at 5 K, excited with 454.5, 457.9, 465.8, and 472.7 nm laser lines, are shown in Figure 5. When 454.5 or 457.9 nm excitation is used, the spectra obtained are essentially similar to the broad-band spectrum obtained at 77 K.¹ However, with 465.8 nm excitation, slightly more intensity appears in the tail of the spectrum. Excitation at 472.7 nm, where the sample hardly absorbs at all, gives a very weak spectrum with a completely different

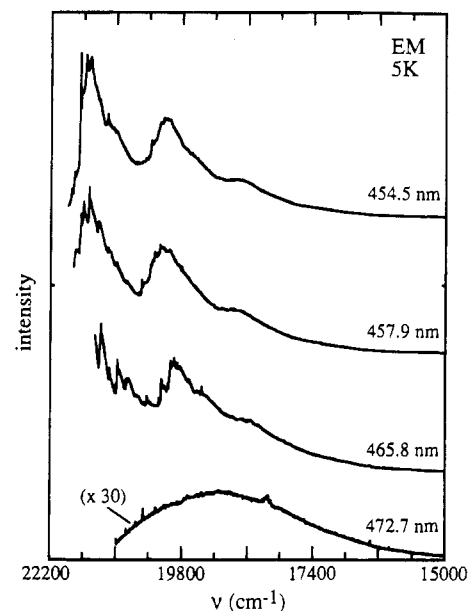


Figure 5. Luminescence spectra of a fresh sample in ethanol–methanol at 5 K, excited at different wavelengths. The excitation wavelength for each spectrum is shown at the right of the curve. The spectrum excited at 472.7 nm has been enlarged to allow comparison of the band shape.

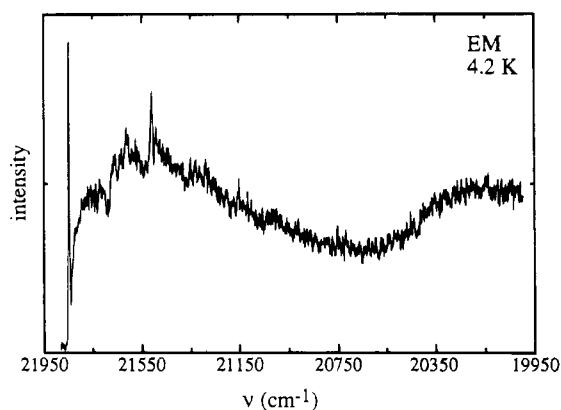


Figure 6. Resonantly-narrowed luminescence spectrum in ethanol–methanol at 4.2 K, excited at 457.9 nm.

appearance; a broad unstructured band with $\nu_{\text{max}} = 19\,120\text{ cm}^{-1}$. Thus a crossover situation seems to apply as the excitation wavelength is increased, changing from structured to broad luminescence. It should be emphasized that the broad emission is very weak indeed for fresh samples, but it was present for all batches of the complex, both triflate and perchlorate salts, which were tested, and also for a sample prepared by dissolving the crystals of the perchlorate salt in EM. Old samples of the complex in EM were found to display the broad luminescence to a much greater degree, so that even the spectrum excited with 457.9 nm had a substantially more intensity in the tail of the luminescence band. These observations point to the presence of decomposition products as possible cause of the unstructured emission which is observed with very low energy excitation.

In Figure 6 the resonantly-narrowed luminescence spectrum of the title compound, excited with 457.9 nm laser light at 4.2 K, is shown. The spectrum exhibits a sharp origin (instrumentally-limited line width 2.9 cm^{-1}), resonant with the laser line at 457.9 nm, followed by a broad vibrational progression. Comparing this spectrum to that of the crystal at the same temperature, it is immediately obvious that there is much more intensity in the unstructured vibrational sideband in EM. This

(22) Riesen, H.; Krausz, E. *Chem. Phys. Lett.* **1990**, 172, 5.

(23) Komada, Y.; Yamauchi, S.; Hirota, N. *J. Phys. Chem.* **1986**, 90, 6425.

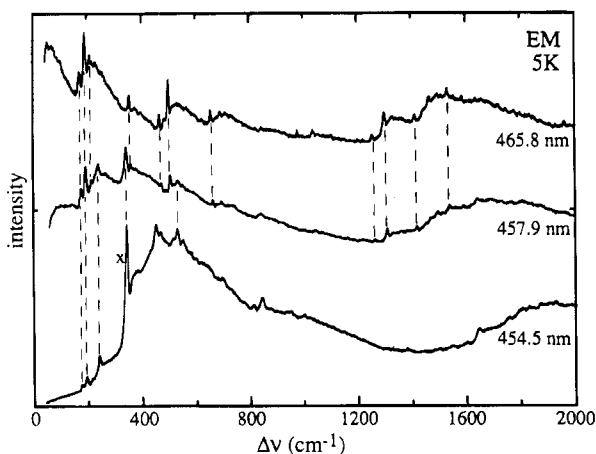


Figure 7. Luminescence spectra in ethanol–methanol at 5 K, showing the high-energy region with vibrational sidelines, excited at different wavelengths (indicated). The spectra have been shifted so that the excitation wavelengths (and therefore origins of the species excited) coincide, to allow comparison of the sidelines. The 337 cm⁻¹ sideline is marked by an x.

might indicate some degree of MLCT character in the luminescence spectrum of the molecule in EM, since the ³MLCT state is known to be close,¹ or could be a result of exciting partly into a sideband in absorption (see below), which would cause a certain amount of non-narrowed luminescence to be observed. When 454.5 nm laser light was used to excite the sample, no resonant origin feature was observed.

Vibrational Sidelines. Figure 7 shows nonresonantly observed, narrowed luminescence spectra of Re(4,7-Me₂phen)(CO)₃py⁺ in EM at 5 K, using 454.5, 457.9, and 465.8 nm excitation. Since there is a much greater degree of inhomogeneous broadening in the glass medium compared to the crystal, the low-energy absorption bands are expected to be quite broad. This allowed the use of several laser lines to excite the sample. In each case the spectrum is that of the subset of molecules which absorb at that particular frequency, and the spectra have been corrected so that the excitation frequencies coincide, to allow comparison of the shifts of the vibrational sidelines. The spectra excited at 465.8 and 457.9 nm have almost all sidelines in common. When 454.5 nm excitation is used, only the low-frequency modes are narrowed. In addition, a very strong feature occurs at $\Delta\nu = 337$ cm⁻¹, with a low-energy phonon wing shifted ≈ 30 cm⁻¹. This band is also present in the 457.9 nm spectrum but is weaker under these conditions. The shift of 337 cm⁻¹ corresponds closely to the frequency of the first strong vibrational sideline in the absorption spectrum of the crystal, at 335 cm⁻¹ (see Figure 2). Presumably, the absorption spectrum of the chromophore in the EM glass at 5 K will be similar to that observed in the crystal, only subjected to much more inhomogeneous broadening. At 454.5 nm, one evidently excites principally into this sideband, and the strong feature in the luminescence spectrum corresponds to the electronic origin of the species which have been selectively excited in this way. Superimposed on this spectrum is also observed the spectrum of the *resonantly* excited species which give the lower frequency sidelines, but the latter are present in a lesser proportion at this wavelength. With 457.9 nm excitation, the observed luminescence occurs predominantly from species which absorb directly into the electronic origin; however the continued presence of the 337 cm⁻¹ feature shows that for some molecules the excitation still involves the sideline. There is no feature at 337 cm⁻¹ in the spectrum excited with 465.8 nm.

We can also compare the vibrational sidelines observed in the luminescence spectrum of the crystal, excited at 454.5 nm,

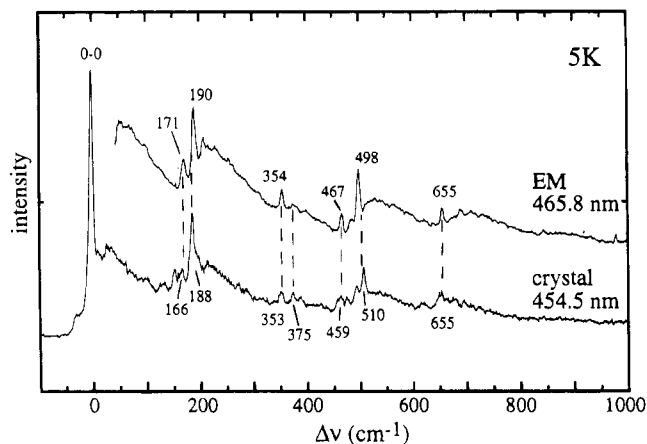


Figure 8. Comparison of the vibrational sidelines in the luminescence of the crystal at 4.2 K (excited at 454.5 nm) and that of the complex in EM at 5 K (excited at 465.8 nm). The spectra have been shifted so that the origins of the chromophores in question coincide, and the frequencies of the major sidelines are shown.

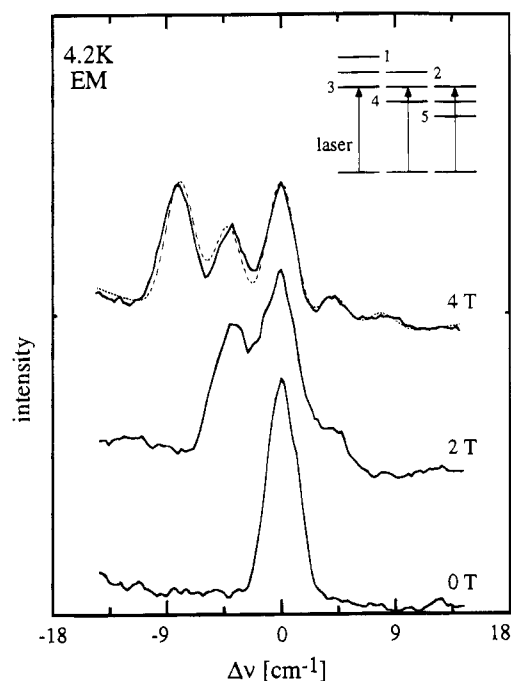


Figure 9. Zeeman effect on the origin of the resonantly-narrowed luminescence of the complex in EM at 4.2 K, excited at 457.9 nm. The magnetic field strength is shown for each spectrum. A calculated spectrum for a field of 4 T is shown by the dashed line. The insert shows how the five-line pattern arises.

with those which are found for the complex in EM, excited at 465.8 nm (Figure 8). The origin transition has been set at 0 cm⁻¹ in each case. The two spectra are strikingly similar and all of the major sidelines are coincident, with low-energy phonon wings associated with the strongest ones. This result shows the strong similarity between the emitting state in the crystal and the principal emitting state in the EM glass. It should be noted that excitation of the crystal at energies lower than the electronic origin (e.g. 472 nm) produced no luminescence at all.

Zeeman Effect. Non-narrowed luminescence spectra of the single crystal and resonantly-narrowed spectra of the complex in EM were measured in a magnetic field at 4.2 K in order to observe the Zeeman splittings in either case. The spectra in EM, at fields of 0, 2, and 4 T are displayed in Figure 9. The splitting of the single origin line into the five-line pattern seen at 4 T is caused by the narrowing effect. For an individual

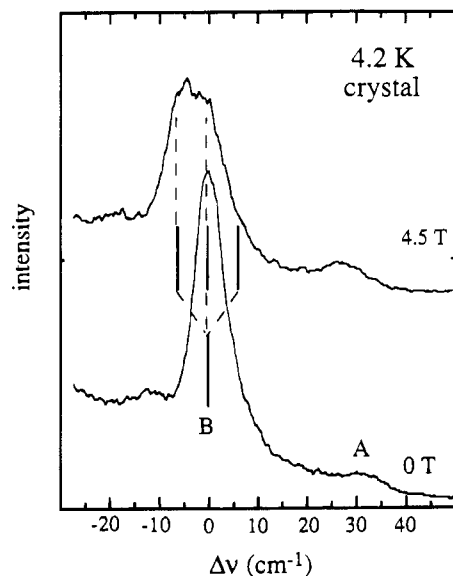


Figure 10. Zeeman effect on the origin of the resonantly-narrowed luminescence of the crystal at 4.2 K, excited at 454.5 nm. A indicates the origin of the bulk material and B indicates the origin of the minority site. The field strength is shown for each spectrum. Lines indicate the estimated splitting of the spin components of origin B in the magnetic field.

molecule, the three components of the spin-triplet excited state become nondegenerate in the presence of the external magnetic field, splitting into the $m_L = +1, 0, -1$ levels. The separation is given by $\Delta E = g\beta B$, where β is the Bohr magneton and B is the magnetic field strength. For a field of 4 T, $\Delta E = 3.74 \text{ cm}^{-1}$ if $g = 2$. The three levels are populated according to a Boltzmann distribution. However, as well as exciting the molecules which have $m_L = 0$ resonant with the laser, one also excites those species within the inhomogeneously broadened absorption which have $m_L = +1$ and $m_L = -1$ resonant. Since ΔE is constant, this leads to five lines, as depicted in Figure 9 (insert). It is possible to calculate the expected energy spacings in the five-line pattern for a given spectrum by simulating the effect of an applied magnetic field on a system of $\approx 10\,000$ molecules having a given zero-field splitting.¹⁴ The calculated spectrum in Figure 9, represented by the dashed line, was obtained by fitting the experimental data to a sum of five Gaussian peaks at the energies derived from the simulation. The simulation required a zero-field splitting ($|D| + |E|$) of $2.5 + 0.5 \text{ cm}^{-1}$ in order to provide a good fit to the experiment.

In the zero-field spectrum of the single crystal (Figure 10), the origin is much broader than in the narrowed EM spectrum (shown in Figure 9), since the crystal has been nonselectively excited. Thus the 4.5 T spectrum is less resolved than could be achieved in the glass. To properly interpret the effect of the applied magnetic field on the intensities in the crystal spectrum, the polarization axes of the chromophore with respect to the field direction and the transition dipole moments for all three spin levels should be known. As there are four molecules in the unit cell of $[\text{Re}(4,7\text{-Me}_2\text{phen})(\text{CO})_3\text{py}](\text{ClO}_4)$ and most of the luminescence occurs from a minority site of unknown symmetry, simulation of the data was not attempted. However, a qualitative interpretation of the results can be given. In a field of 4.5 T the origin is clearly broadened in comparison to the zero-field spectrum, due to the splitting of the three spin components. A magnetic field dependence can also be seen to operate in the weak origin A, and one can discern that the shifts and intensity redistribution are similar to the behavior found for origin B. Such behavior is consistent with a ^3LC emitting state which has relatively small zero-field splittings. The

Table 4. Lifetimes of $[\text{Re}(4,7\text{-Me}_2\text{phen})(\text{CO})_3\text{py}]^+$ ^a

	298 K	77 K	10 K	77 K ^b
EM	4.3	17 ^c	49 ^c	11.3
crystal	9.8	83 (25%) 10.8	140 (5%) ≈ 10	

^a Excitation at 460 nm, detected at 530 nm, in μs . ^b Excitation at 472 nm. ^c Dual exponential.

estimated positions of the three components in the magnetic field is shown for origin B in Figure 10.

Decay Characteristics. In room-temperature fluid solutions, as has been reported earlier,¹ the title complex displays exponential decay of the luminescence and has a rather long excited-state lifetime of $7 \mu\text{s}$ in CH_2Cl_2 . Anomalous behavior occurs in frozen glasses where the decay becomes strongly nonexponential, having a short-lived component of $\approx 20 \mu\text{s}$ and a long-lived component of $\approx 90 \mu\text{s}$ with excitation at 355 nm. Time-resolved spectra demonstrated that luminescence spectra detected at short times after the laser pulse had more intensity in the tail of the vibrational progression, and the structure became more defined as the delay time was increased. This was taken as an indication that the structured luminescence was derived from a ^3LC state, whereas the broader emission originated from a $^3\text{MLCT}$ state. Steady-state luminescence spectra, excited using a xenon lamp, were structured and similar in appearance to the time-resolved spectra detected at long delay times.¹

Decay times measured using different excitation (and detection) wavelengths are shown in Table 4, for both crystal and EM samples. In EM at 77 K the luminescence is long-lived and decays nonexponentially with excitation at wavelengths of 460 nm and below. Parameters obtained from fitting routines are frequently suspect in cases where multiexponential decay is observed; however we can advance a qualitative interpretation of the changes in going from 77 K to 10 K. With excitation at $\approx 460 \text{ nm}$, a fit of the decay profile at 77 K gives 16 and $83 \mu\text{s}$ for a dual exponential, with initial amplitudes of 75% and 25% respectively. At 10 K, the decays are much closer to single exponential, and the fit gives 50 and $140 \mu\text{s}$ with initial amplitudes of 95% and 5%. Two factors need to be considered here. First, the decays of ^3LC states can become significantly nonexponential at liquid helium temperatures,²⁴ because the spin sublevels of the triplet, usually separated by $< 1 \text{ cm}^{-1}$, are no longer thermalized. This often leads to multiexponential decay profiles where the major component is shorter-lived than the average for the three levels, and there is also a minor, longer-lived component. Second, the lifetimes of $^3\text{MLCT}$ emitting states typically have a strong temperature dependence over this range, becoming much longer at lower temperatures. Therefore we do not assign the two lifetimes obtained from a dual-exponential fit to a particular type of emission. It appears likely from the data that the shorter-lived ^3LC level(s) and the $^3\text{MLCT}$ emission have comparable decay rates at 10 K, and these together constitute the shorter decay parameter obtained from the fit. The longer-lived ^3LC level(s) accounts for the weak component of $140 \mu\text{s}$ at 10 K. A recent study of very similar Re(I) complexes which display $^3\text{MLCT}$ luminescence at all temperatures gave excited-state lifetimes of $\approx 50 \mu\text{s}$ for $\text{Re}(\text{bpy})(\text{CO})_3\text{Cl}$ and $80 \mu\text{s}$ for $\text{Re}(\text{phen})(\text{CO})_3\text{Cl}$ at $\approx 10 \text{ K}$,²⁵ which are in good agreement with the value for the short component in the decays of $[\text{Re}(4,7\text{-Me}_2\text{phen})(\text{CO})_3\text{py}]^+$ at 10 K.

With 472 nm excitation, which produces the weak broad emission spectrum in Figure 5, the decay is single exponential

(24) Krausz, E.; Higgins, J.; Riesen, H. *Inorg. Chem.* **1993**, *32*, 4053.

(25) Striplin, D. R.; Crosby, G. A. *Chem. Phys. Lett.* **1994**, *221*, 426.

with a lifetime of 11.3 μs at 77 K when detected at 530 nm. As discussed earlier, this could be attributed to excitation of the red edge of the ³MLCT absorption or to the presence of decomposition products or impurities.

Little information can be gleaned from the lifetime measurements on the crystal. Due to the energy transfer which occurs in the neat material, the decay time remains roughly constant over the entire temperature range 5–298 K. It would be preferable to perform the experiments on a dilute crystal, if a suitable host material could be found.

Discussion

The results obtained from measurements on the single crystal are all entirely consistent with a ³LC assignment for the lowest excited state. The appearances of the absorption and emission spectra alone are compelling evidence for this assignment. Luminescence occurs from a minority site within the crystal at 4.2 K, due to fast energy transfer processes which occur in the neat sample. The absorption spectrum represents the bulk crystal and is in itself strong evidence for the ³LC assignment of the lowest excited state. Thus we can infer that although there are different sites in the crystal, the chromophores are very close in energy (within 30 cm⁻¹) and are of similar character. As the origin carries most of the intensity, the equilibrium geometries of the ground and excited states must be very similar. The Zeeman results demonstrate that the emitting state is a spin triplet and the zero-field splitting is relatively small. Thus in the rigid, relatively homogeneous environment of the single crystal, luminescence occurs from the lowest ³LC state of the chromophore.

Essentially, the results obtained from frozen EM samples demand a ³LC assignment for the emitting state in this environment as well. Again, the origin carries a significant portion of the luminescence intensity, the spectra are structured, and, most compelling, the Zeeman experiment shows the zero-field splitting is relatively small (≈2.5 cm⁻¹), consistent with a perturbed spin triplet. However all transitions suffer much more from inhomogeneous broadening in a glass matrix compared to a crystal, and this leads to some complications. From comparison of the vibrational sidelines which are produced with 465.8, 457.9, and 454.5 nm excitation at 5 K, it is evident that in absorption there is an overlap between the inhomogeneously-broadened origin line and the strong vibrational feature which lies 335 cm⁻¹ higher in energy. At 454.5 nm one excites mainly into this sideband and thus obtains the spectrum of the species which have their origins 335 cm⁻¹ from this wavelength. Only a few species have their origin actually at 454.5 nm, which corresponds to the high-energy limit of the inhomogeneously-broadened origin band. Lower energy laser lines give direct excitation of the origin for the majority of molecules.

In comparison with zero-field splittings reported for similar transition-metal complexes which display ³LC luminescence, the value of 2.5 cm⁻¹ for [Re(4,7-Me₂phen)(CO)₃py]⁺ is rather high. [Rh(bpy)₃]³⁺, [Rh(phen)₃]³⁺, and [Rh(phen)₂(CN)₂]³⁺^{23,26} have maximum zero-field splittings of 0.1–0.2 cm⁻¹, similar to the splitting of the free phenanthroline ligand, and [Ru(i-biq)₃]²⁺²⁴ (i-biq = bisoquinoline) and [Ir(phen)₃]³⁺²⁷ also have zero-field splittings of <1 cm⁻¹. The Ir(III) complex may provide the best analogy to the present case, as rhenium and iridium are both third-row metals. The large zero-field splitting in [Re(4,7-Me₂phen)(CO)₃py]⁺ could simply be a result of the heavy atom effect of the Re(I) center. However it is known

that the lowest ³MLCT state is close in energy to the ³LC in this complex.¹ In addition, the nonexponential decay kinetics at 77 K and the time-resolved spectra measured previously¹ indicated a considerable degree of ³MLCT character in the emission. It therefore seems likely that the ³LC emitting state is perturbed by the ³MLCT state. This might result in an increased orbital contribution to the spin triplet, which would be manifested in rather large zero-field splittings. For [Ir(5,6-Me₂phen)₂Cl₂]⁺, Zeeman experiments established that the luminescence originated from the lowest ³LC state of the molecule, but the spin triplet was significantly perturbed by the proximity of the ³MLCT state.¹⁴ The dual-exponential decay kinetics of this complex were attributed to the existence of a range of ³LC/³MLCT energy gaps caused by the inhomogeneous environment, where a smaller separation resulted in a more perturbed ³LC emitting state and therefore a shorter lifetime. We believe that an analogous situation prevails for [Re(4,7-Me₂phen)(CO)₃py]⁺ and that this accounts for the multiple-exponential decays, time-dependent luminescence spectra, and other unusual behaviors which are observed for this complex.

A related possibility should also be considered. Since a range of ³MLCT/³LC energy gaps are certainly found in EM, there may be a percentage of molecules for which the ³MLCT state is at lower energy, although the ³LC state is clearly lowest on average, as it dominates the luminescence at all excitation wavelengths where the sample has a reasonable absorbance. For example, in the mixed-ligand complexes [Ir(bpy)₂(phen)]³⁺ and [Ir(phen)₂(bpy)]³⁺,²⁴ the biexponential luminescence decay profiles were found to result from an overlap of the absorption bands involving the bpy and phen ligands, where phen was lower in energy on average but a significant proportion of the molecules in the overlap region had bpy lower. Thus, both phen- and bpy-based emission was observed from these samples. The broad, weak luminescence observed with 472.7 nm excitation at 77 or 5 K might be the result of selective excitation of only ³MLCT emitters in the EM glass, if the tail of the MLCT absorption protrudes beyond that of the ³LC band. If the ³MLCT absorption were broader than the ³LC, as is likely, it would be possible to select the low-energy tail of this band with the appropriate excitation frequency. However, as there is definitely a decomposition product which luminesces at about this energy, one is cautious about assigning this band to the complex itself.

Alternatively, one could be observing "dual emission", the phenomenon in which emission from either of two non-thermally-equilibrated states is possible for a given molecule. For a population of molecules, one sees both types occurring in a ratio which is governed by the degree to which the excitation energy is partitioned. A few organic molecules have been proved to luminesce from two nonequilibrated states simultaneously,²⁸ as have some transition-metal ions doped in inorganic solids,²⁹ but in these cases the energy gap between the emitting states is very large (>5000 cm⁻¹). The occurrence of genuine dual emission from close-lying states has yet to be established *unequivocally* for the complexes of transition metals which have been examined. This issue has been rather a controversial one. The problem is that the behavior of a population of dual emitters would closely parallel that of two distinct molecules, so that most experimental techniques which are applied to the study of such species could not discriminate between the two cases. The techniques employed here are no exception.

(26) Miki, H.; Shimada, M.; Azumi, T.; Brozik, J. A.; Crosby, G. A. *J. Phys. Chem.* **1993**, *97*, 11175.

(27) Riesen, H.; Krausz, E. *J. Lumin.* **1992**, *53*, 263.

(28) Birks, J. B. *Photophysics of Aromatic Molecules*; Wiley: New York, 1970.

(29) Ferguson, J.; Masui, H. *J. Phys. Soc. Jpn.* **1977**, *42*, 1640.

Several circumstantial observations suggest that the inhomogeneous distribution is at least the primary, if not the sole, cause of the dual-emission phenomenon in the present case and possibly in other examples. First, the title complex gives purely ^3LC emission from a single crystal, which can be considered to be approximately homogeneous. In addition, the sample gives nonexponential decay kinetics at room temperature, where thermalization would be expected to be complete, when dissolved in a polymer film.³⁰ The inhomogeneous broadening in polymer films is acknowledged to be considerably worse than it is in organic glasses like ethanol–methanol. Finally, it is worth considering that all of the examples of dual emission from transition-metal complexes so far have occurred for samples embedded in solid, amorphous hosts. This is not to dismiss the possibility of simultaneous emission from close-lying states which are not in thermal equilibrium but rather to emphasize the role of sample inhomogeneity in causing many of the effects associated with its apparent occurrence.

Conclusions

In single crystals of $[\text{Re}(4,7\text{-Me}_2\text{phen})(\text{CO})_3\text{py}]\text{ClO}_4$, the luminescence occurs from a ^3LC excited state. When the complex is dissolved in ethanol–methanol glass, the lumines-

cence also occurs from a ^3LC state, but a contribution from the $^3\text{MLCT}$ state is also evident. The unusually large zero-field splitting of the origin indicates that the ^3LC emitting state is perturbed by the nearby $^3\text{MLCT}$ state. The extent of the perturbation is likely to be dependent on the magnitude of the energy gap between the two states. Since the inhomogeneous EM matrix produces a range of $^3\text{LC}/^3\text{MLCT}$ energy gaps, this accounts for the nonexponential decay profiles which are found in the EM samples. It is also possible that in the amorphous glass some chromophores have the $^3\text{MLCT}$ lower, but these species would constitute a minority. To our knowledge this is the first example of luminescence line narrowing in a $\text{Re}(\text{I})$ tricarbonyl complex.

Acknowledgment. We are deeply grateful to Dr. Hans Riesen for his advice and assistance in the line-narrowing experiments and to Dr. Elmars Krausz for helpful discussions. We thank the Office of Basic Energy Sciences of the Department of Energy for support and Jonathan Pollitte of the University of Tennessee for his assistance in obtaining the X-ray data.

Supplementary Material Available: Tables of data collection and refinement parameters, bond distances, bond angles, anisotropic thermal parameters, and hydrogen atom positions (5 pages). Ordering information is given on any current masthead page.

(30) Wallace, L. Unpublished observations.